

Quantum Spin Hall Effect in Silicene and Two-Dimensional Germanium

Cheng-Cheng Liu, Wanxiang Feng, and Yugui Yao*

*Beijing National Laboratory for Condensed Matter Physics and Institute of Physics,
Chinese Academy of Sciences, Beijing 100190, China
(Received 18 April 2011; published 9 August 2011)*

We investigate the spin-orbit opened energy gap and the band topology in recently synthesized silicene as well as two-dimensional low-buckled honeycomb structures of germanium using first-principles calculations. We demonstrate that silicene with topologically nontrivial electronic structures can realize the quantum spin Hall effect (QSHE) by exploiting adiabatic continuity and the direct calculation of the Z_2 topological invariant. We predict that the QSHE can be observed in an experimentally accessible low temperature regime in silicene with the spin-orbit band gap of 1.55 meV, much higher than that of graphene. Furthermore, we find that the gap will increase to 2.9 meV under certain pressure strain. Finally, we also study germanium with a similar low-buckled stable structure, and predict that spin-orbit coupling opens a band gap of 23.9 meV, much higher than the liquid nitrogen temperature.

DOI: 10.1103/PhysRevLett.107.076802

PACS numbers: 73.43.-f, 71.70.Ej, 73.22.-f, 85.75.-d

Recent years have witnessed great interest [1–6] in the quantum spin Hall effect (QSHE), a new quantum state of matter with a nontrivial topological property, due to its scientific importance as a novel quantum state and the technological applications in spintronics. This novel electronic state with time-reversal invariance is gapped in the bulk and conducts charge and spin in gapless edge states without dissipation at the sample boundaries. The existence of QSHE was first proposed by Kane and Mele in graphene in which the spin-orbit coupling (SOC) opens a band gap at the Dirac point [1]. Subsequent works, however, showed that the SOC is rather weak, which is in fact a second order process for graphene, and the QSHE in graphene can occur only at an unrealistically low temperature [7–9]. So far, there is only one proposal that is able to demonstrate QSHE in a real system, which is in two-dimensional HgTe-CdTe semiconductor quantum wells [3,4] in spite of some theoretic suggestions [5,6].

Nevertheless, HgTe quantum wells have serious limitations such as toxicity, difficulty in processing, and incompatibility with current silicon-based electronic technology. As the counterpart of graphene [10] for silicon, silicene recently synthesized has shown that a low-buckled two-dimensional hexagonal structure corresponds to a stable structure, and there is also evidence of a graphenelike electronic signature in silicene nanoribbons experimentally [11–13]. Therefore, almost every striking property of graphene could be transferred to this innovative material with the extra advantage of easily being incorporated into the silicon-based microelectronics industry.

In this Letter we provide systematic investigations on the spin-orbit gap in silicene and germanium with two-dimensional honeycomb geometry by first-principles calculation, and show that an appreciable gap can be opened at the Dirac points due to spin-orbit coupling and the low-buckled structure. We predict that QSHE can be observed

in an experimentally accessible temperature regime in both systems. Further, we find the strain can tune gap size. Our argument is based on adiabatic continuity of the band structures of the stable low-buckled geometry to the topologically nontrivial planar silicene with QSHE, then confirmed by direct calculation of the Z_2 topological invariant.

The structure of silicene is shown in Fig. 1. We obtain the low-buckled geometry of minimum energy and stability with lattice constant $a = 3.86 \text{ \AA}$ and nearest neighbor Si-Si distance $d = 2.28 \text{ \AA}$ through structural optimization and calculations of phonon spectrum. The results agree with the previous calculations [14,15]. Compared with graphene, the larger Si-Si interatomic distance weakens

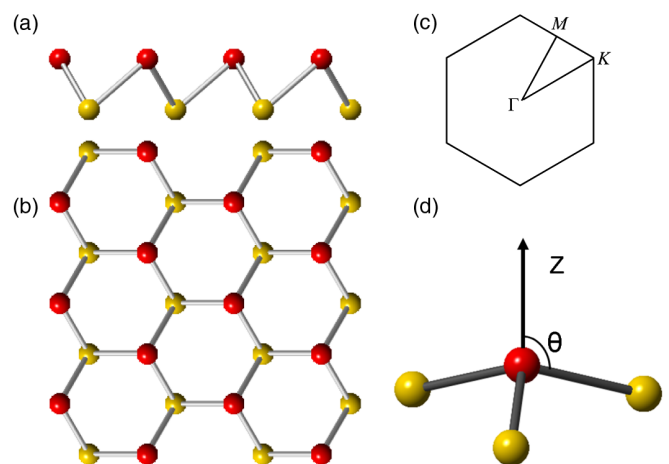


FIG. 1 (color online). The lattice geometry of low-buckled silicene. (a), (b) The lattice geometry from the side view and top view, respectively. Note that A sublattice (red or gray) and B sublattice (yellow or light gray) are not coplanar. (c) The first Brillouin zone of silicene and its points of high symmetry. (d) The angle θ is defined as being between the Si-Si bond and the Z direction normal to the plane.

the π - π overlaps, so it cannot maintain the planar structure anymore. This results in a low-buckled structure with sp^3 -like hybrid orbitals. In Fig. 1(d), one can define the angle θ between the Si-Si bond and the direction normal to the plane. The sp^2 (planar), low-buckled, and sp^3 configurations correspond to $\theta = 90^\circ$, $\theta = 101.73^\circ$, and $\theta = 109.47^\circ$, respectively.

To illustrate the band topology of the low-buckled silicene, we begin with their graphene analog, planar silicene, and follow its band structure under an adiabatic transformation during which the unstable planar honeycomb structure is gradually evolved into the low-buckled honeycomb structure. Planar silicene with the same structure as graphene should have similar properties. Furthermore, since Si atoms have greater intrinsic spin-orbit coupling strength than C atoms, it is natural to conceive that the quantum spin Hall effect is more significant in planar silicene. According to symmetry, the low energy effective Hamiltonian with SOC in planar silicene in the vicinity of Dirac point K can be described by

$$H_{\text{eff}}^{[K]} \approx \begin{pmatrix} -\xi\sigma_z & v_F(k_x + ik_y) \\ v_F(k_x - ik_y) & \xi\sigma_z \end{pmatrix}, \quad (1)$$

where v_F is the Fermi velocity of π electrons near the Dirac points with the almost linear energy dispersion, and σ_z is Pauli matrix. The effective SOC ξ for planar silicene has the explicit form $\xi \approx 2\xi_0^2|\Delta_\epsilon|/(9V_{sp\sigma}^2)$ with Δ_ϵ being the energy difference between the $3s$ and $3p$ orbitals and ξ_0 half the intrinsic spin-orbit coupling strength, respectively [7]. The parameter $V_{sp\sigma}$ corresponds to the σ bond formed by the $3s$ and $3p$ orbitals. The effective Hamiltonian near Dirac point K^* can be obtained by the time-reversal operation on the one near K . The above equation results in a spectrum $E(\vec{k}) = \pm\sqrt{(v_F k)^2 + \xi^2}$. Therefore, one can estimate the energy gap, which is 2ξ at the Dirac points, to be about the order of 0.1 meV by taking the values of the corresponding parameters [16]. Notice that in planar silicene ($\theta = 90^\circ$) π orbitals and σ orbitals are coupled only through the intrinsic SOC. So, the effective SOC is in fact a second order process. However, with the deviation ($\theta > 90^\circ$) from the planar geometry, π orbitals and σ orbitals can also directly hybridize. Consequently, the magnitude of the effective SOC depends on the angle θ . As can be expected with increasing the degree of deviation from the planar structure, the effective SOC will be incremental, and QSHE will be more significant.

The argument above is supported by our first-principles calculations based on density-functional theory (DFT). The relativistic electronic structure of silicene is obtained self-consistently by using the projector augmented wave (PAW) pseudopotential method implemented in the VASP package [17]. The exchange-correlation potential is treated by Perdew-Burke-Ernzerhof (PBE) potential [18].

We carry out detailed and systematic calculations of the band structure in adiabatic evolution from the planar

honeycomb geometry to the low-buckled honeycomb geometry. The evolution of the gap opened by SOC for the π orbital at the Dirac point K from the planar honeycomb geometry to the low-buckled honeycomb geometry is shown in Fig. 2(a). Figures 2(b) and 2(d) show the band structures of planar and low-buckled silicene, respectively, with the corresponding structures in Fig. 2(a). The band structures of planar and low-buckled geometry are slightly different, except linear dispersion near the Fermi level [14,19]; in consideration of that the gap induced by the effective SOC increases and the degeneracies split at some k points. The difference of both the band structures in the vicinity of the Γ point and in the energy range from -3 to -2 eV actually means that σ orbital and π orbital can directly hybridize only in low-buckled geometry. We can find that the gap induced by SOC for σ orbitals is 34.0 meV at the Γ point in both geometries. As is also shown in the figure that the magnitude of the gap induced by effective SOC for the π orbital at the K point in planar geometry is 0.07 meV, which is in agreement with the

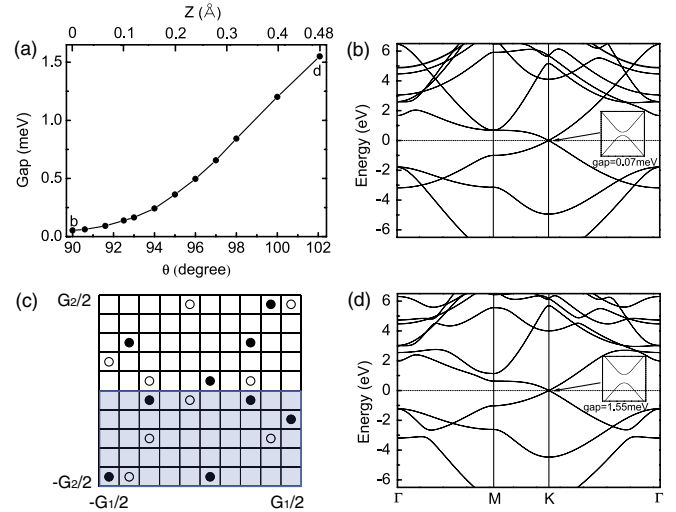


FIG. 2 (color online). The adiabatic evolution of the gap, calculated relativistic band structure, and the topological Z_2 invariant of silicene. (a) The evolution of the gap opened by SOC for the π orbital at the Dirac point K from the planar honeycomb geometry to the low-buckled honeycomb geometry with keeping the Si-Si bond length constant. The top and bottom abscissas correspond to the difference of vertical height between A sublattice and B sublattice and the θ angle aforementioned, respectively, during evolution. (b) and (d) are the relativistic band structures with the corresponding geometries in (a). (b),(d) Main panel: the relativistic band structure of planar silicene and low-buckled silicene, respectively. Inset: zooming in the energy dispersion near the K point and the gap induced by SOC. (c) The n -field configuration for silicene. The calculated torus in Brillouin zone is spanned by G_1 and G_2 . Note that the two reciprocal lattice vectors form an angle of 120° . The white and black circles denote $n = 1$ and -1 , respectively, while the blank denotes 0. The Z_2 invariant is 1 obtained by summing the n field over half of the torus.

estimate obtained from the tight-binding model discussed above. In the low-buckled structure, the magnitude of the gap is 1.55 meV, which corresponds to 18 K. The top coordinate in Fig. 2(a) denotes the altitude difference of two nonequivalent Si atoms within a primitive cell in the vertical direction. The figure indicates that the gap with the magnitude of 0.07 meV in the planar structure has been increasing to 1.55 meV in the low-buckled structure with energy minimum and stability. Most importantly, the gap is not closed. Therefore, the low-buckled silicene with energy minimum and stability must share the same nontrivial topological properties as the planar silicene. Consequently, QSHE can be realized in the low-buckled silicene, namely, the native geometry of silicene. The argument can be confirmed by direct calculation of the Z_2 topological invariant.

One can interpret nonzero topological Z_2 invariant as an obstruction to make the wave functions smoothly defined over half of the entire Brillouin zone under a certain gauge with the time-reversal constraint [20–22]. The band topology can be characterized by the Z_2 invariant. $Z_2 = 1$ characterizes a nontrivial band topology while $Z_2 = 0$ means a trivial band topology. Here we follow the method in Ref. [23] to directly perform the lattice computation of the Z_2 invariants from our first-principles method [24,25]. The n -field configuration for the low-buckled silicene is shown in Fig. 2(c) from first-principles calculations. It should be noted that different gauge choices result in different n -field configurations; however, the sum of the n field over half of the Brillouin zone is gauge invariant module 2, namely Z_2 topological invariant. As shown in Fig. 2(c), low-buckled silicene has nontrivial band

topology with the topological invariant $Z_2 = 1$. Therefore, QSHE can be realized in the low-buckled silicene, that is the native geometry of silicene.

In what follows, we investigate the gap opened by SOC at Dirac points related to QSHE and the Fermi velocity of charge carriers v_F near the Dirac points in a series of silicene geometries under hydrostatic strain from the first-principles method. We find that while the largest pressure strain can reach -6% without destroying the nontrivial topological properties of those systems, the magnitude of the gap at Dirac points induced by SOC can be up to 2.90 meV, which corresponds to 34 K. As shown in Fig. 3, the magnitude of the gap at Dirac points induced by SOC is incremental with the decrease of hydrostatic strain Δ , which is defined as $\Delta = (a - a_0)/a_0 \times 100\%$, with a_0 and a being the lattice constant without and with hydrostatic strain, respectively. In the pressure strain range, the QSHE can be also realized in the system and even more pronounced. The figure also indicates that the greater the angle θ , the greater the gap. In addition, we evaluate the Fermi velocity of charge carriers v_F near the Dirac points under different hydrostatic strain and find that the magnitude of the hydrostatic strain does not significantly change the carrier Fermi velocity v_F . The value is slightly less than the typical value in graphene, say, 10^6 m/s due to the larger Si-Si atomic distance.

Recently, several experiments on silicene have been reported [11–13]. They have not only proven silicene adopting slightly buckled honeycomb geometry and possessing the band dispersion with a behavior analogous to the Dirac cones of graphene, but also synthesized a silicene sheet through epitaxial growth. With the advancement in experimental techniques, we expect that silicene with high quality will soon be manufactured. The experimental data available can be compared with our theoretical prediction, then.

Although germanium with two-dimensional honeycomb geometry has not yet been synthesized in experiments, we also conduct a detailed study on germanium with two-dimensional honeycomb structure because of its similarity to the other group IVA elements in the periodic table, as well as its significant importance as semiconductor material. After structural optimization and calculations of phonon spectrum, the low-buckled geometry of minimum energy and stability with lattice constant $a = 4.02$ Å and nearest neighbor Ge-Ge distance $d = 2.42$ Å is obtained. As shown in Figs. 4(a) and 4(b), Ge with low-buckled honeycomb structure is insulator while Ge with planar honeycomb structure is metallic. Figure 4(b) indicates that the magnitude of the gap induced by effective SOC for the π orbital at the K point in low-buckled geometry is 23.9 meV corresponding to 277 K which is much higher than the liquid nitrogen temperature. The direct calculation for topological Z_2 invariant proves that Ge with low-buckled honeycomb structure has nontrivial band topology. Therefore, we predict that QSHE will be realized in native

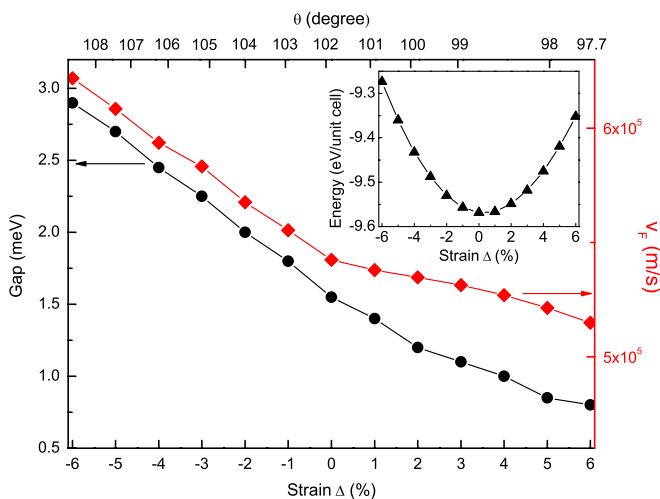


FIG. 3 (color online). The gap induced by SOC and the Fermi velocity of charge carriers v_F near the Dirac points are calculated from the first-principles method under different hydrostatic strain conditions. The black circles and red or gray diamonds mark the gap and the Fermi velocity v_F near the Dirac points under different hydrostatic strain Δ . Inset: Energy of unit cell versus different hydrostatic strain condition.

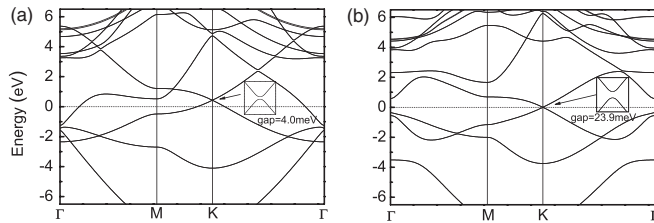


FIG. 4. The calculated relativistic band structure of germanium with honeycomb structure. (a),(b) Main panel: the relativistic band structure of germanium with planar and low-buckled honeycomb structure, respectively. Inset: zooming in the energy dispersion near the K point and the gap induced by SOC.

germanium with two-dimensional low-buckled honeycomb geometry and easily observed experimentally once this novel material is synthesized.

In conclusion, we have shown both silicene and Ge with two-dimensional honeycomb geometry have nontrivial topological properties in their native structure. In addition, the QSHE in silicene can be more significant under a range of hydrostatic strain due to the increasing gap size. These are confirmed by direct calculations of the topological Z_2 invariants from first-principles methods. Silicene and Ge with low-buckled honeycomb geometry have novel physical properties akin to graphene such as the linear energy dispersion at the Fermi level. Besides, silicene and Ge with low-buckled geometry and great SOC can be not only synthesized and processed using mature semiconductor techniques but also more easily integrated into the current electronics industry. All of these make silicene and Ge with low-buckled honeycomb geometry cornucopias of fundamental scientific interest and promising applications.

This work was supported by NSF of China (Grant No. 10974231), the MOST Project of China (Grants No. 2007CB925000 and 2011CBA00100), and Supercomputing Center of Chinese Academy of Sciences.

*To whom correspondence should be addressed.

ygyao@aphy.iphy.ac.cn

- [1] C. L. Kane and E. J. Mele, *Phys. Rev. Lett.* **95**, 226801 (2005).
- [2] C. L. Kane and E. J. Mele, *Phys. Rev. Lett.* **95**, 146802 (2005).
- [3] B. A. Bernevig, T. L. Hughes, and S. C. Zhang, *Science* **314**, 1757 (2006).

- [4] M. König, S. Wiedmann, C. Brüne, A. Roth, H. Buhmann, L. W. Molenkamp, X. L. Qi, and S. C. Zhang, *Science* **318**, 766 (2007).
- [5] S. Murakami, *Phys. Rev. Lett.* **97**, 236805 (2006).
- [6] C. X. Liu, T. L. Hughes, X. L. Qi, K. Wang, and S. C. Zhang, *Phys. Rev. Lett.* **100**, 236601 (2008).
- [7] Y. G. Yao, F. Ye, X. L. Qi, S. C. Zhang, and Z. Fang, *Phys. Rev. B* **75**, 041401(R) (2007).
- [8] D. Huertas-Hernando, F. Guinea, and A. Brataas, *Phys. Rev. B* **74**, 155426 (2006).
- [9] H. Min, J. E. Hill, N. A. Sinitsyn, B. R. Sahu, and L. Kleinman, A. H. MacDonald, *Phys. Rev. B* **74**, 165310 (2006).
- [10] A. K. Gelm and K. S. Novoselov, *Nature Mater.* **6**, 183 (2007).
- [11] B. Aufray, A. Kara, S. Vizzini, H. Oughaddou, C. Léandri, B. Ealet, and G. L. Lay, *Appl. Phys. Lett.* **96**, 183102 (2010).
- [12] P. E. Padova, C. Quaresima, C. Ottaviani, P. M. Sheverdyeva, P. Moras, C. Carbone, D. Topwal, B. Olivieri, A. Kara, H. Oughaddou, B. Aufray, and G. L. Lay, *Appl. Phys. Lett.* **96**, 261905 (2010).
- [13] B. Lalmi, H. Oughaddou, H. Enriquez, A. Kara, S. Vizzini, B. Ealet, and B. Aufray, *Appl. Phys. Lett.* **97**, 223109 (2010).
- [14] S. Cahangirov, M. Topsakal, E. Aktürk, H. Sahin, and S. Ciraci, *Phys. Rev. Lett.* **102**, 236804 (2009).
- [15] Y. Ding and J. Ni, *Appl. Phys. Lett.* **95**, 083115 (2009).
- [16] W. A. Harrison, *Electronic Structure and the Properties of Solids*, 46-51 (W. H. Freeman and Company, San Francisco, 1980).
- [17] G. Kresse and J. Furthmüller, *Phys. Rev. B* **54**, 11 169 (1996).
- [18] J. P. Perdew, K. Burke, and M. Ernzerhof, *Phys. Rev. Lett.* **77**, 3865 (1996).
- [19] G. G. Guzmán-Verri and L. C. Lew Yan Voon, *Phys. Rev. B* **76**, 075131 (2007).
- [20] L. Fu and C. L. Kane, *Phys. Rev. B* **74**, 195312 (2006).
- [21] J. E. Moore and L. Balents, *Phys. Rev. B* **75**, 121306(R) (2007).
- [22] D. Xiao, M. C. Chang, and Q. Niu, *Rev. Mod. Phys.* **82**, 1959 (2010).
- [23] T. Fukui and Y. Hatsugai, *J. Phys. Soc. Jpn.* **76**, 053702 (2007).
- [24] D. Xiao, Y. G. Yao, W. X. Feng, J. Wen, W. G. Zhu, X. Q. Chen, G. M. Stocks, and Z. Y. Zhang, *Phys. Rev. Lett.* **105**, 096404 (2010).
- [25] W. X. Feng, D. Xiao, J. Ding, and Y. G. Yao, *Phys. Rev. Lett.* **106**, 016402 (2011).